Demonstration by FRET of BACE interaction with the amyloid precursor protein at the cell surface and in early endosomes

Ayae Kinoshita, Hiroaki Fukumoto, Tejal Shah, Christa M. Whelan, Michael C. Irizarry and Bradley T. Hyman*

Alzheimer Disease Research Laboratory, Massachusetts General Hospital, Harvard Medical School, Charlestown, MA 02129, USA
*Author for correspondence (e-mail: bhyman@partners.org)

Accepted 30 April 2003
Journal of Cell Science 116, 3339-3346 © 2003 The Company of Biologists Ltd
doi:10.1242/jcs.00643

Summary

Amyloid-β peptide, which accumulates in senile plaques in Alzheimer's disease, is derived from the amyloid precursor protein (APP) by proteolytic processing. β-secretase (Asp2), which cleaves APP at the N-terminus of amyloid-β, has recently been identified to be the protease BACE. In the present study, we examined the subcellular localization of interactions between APP and BACE by using both double immunofluorescence and a fluorescence resonance energy transfer (FRET) approach. Cell surface APP and BACE, studied by using antibodies directed against their ectodomains in living H4 neuroglioma cells co-transfected with APP and BACE, showed exquisite co-localization and demonstrated a very close interaction by FRET analysis. The majority of cell surface APP and BACE were internalized after 15 minutes, but they remained strongly co-localized together in the early endosomal compartment, where FRET analysis demonstrated a continued close interaction. By contrast, at later timepoints, almost no co-localization or FRET was observed in lysosomal compartments. To determine whether the APP-BACE interaction on cell surface and endosomes contributed to amyloid-β synthesis, we labeled cell surface APP and demonstrated detectable levels of labeled amyloid-β within 30 minutes. APP-Swedish mutant protein enhanced amyloid-β synthesis from cell surface APP, consistent with the observation that it is a better BACE substrate than wild-type APP. Taken together, these data confirm a close APP-BACE interaction in early endosomes, and highlight the cell surface as an additional potential site of APP-BACE interaction.

Key words: Alzheimer's disease, Amyloid-β peptide, Amyloid precursor protein, BACE, Co-localization, Fluorescence resonance energy transfer, Endocytosis

Introduction

The pathologic hallmarks of Alzheimer's disease are senile plaques and neurofibrillary tangles. Senile plaques are primarily made up of deposits of amyloid-β protein, a proteolytic product derived from the larger amyloid precursor protein (APP) (for a review, see Selkoe, 1998; DeStrooper and Annaert, 2000). APP is a large single transmembrane domain molecule inserted into the endoplasmic reticulum, transported to the Golgi apparatus, to the cell surface, and recycled by endocytosis to endosomes. It is not yet fully understood where amyloid-β is generated. However, the molecular identification of the secretase activities that cleave the amyloid-β peptide from the transmembrane and adjacent extracellular domains of APP to yield the 4-kDa amyloid-β product provides an opportunity to examine secretase-APP interactions in specific cell compartments in vitro. β-cleavage, which sheds the majority of the ectodomain of APP, leaving behind a 99 amino acid stump that includes the transmembrane domain, is mediated by BACE (or Asp2) (Vassar et al., 1999; Shinha et al., 1999; Yan et al., 1999). This short carboxyl terminal APP is a substrate for gamma secretase, an enzyme that mediates an intramembranous cleavage resulting in a 40 or 42 amino acid amyloid-β peptide. Overexpression of BACE in transgenic mice leads to enhanced generation of amyloid-β (Bodendorf et al., 2002), whereas BACE null mice produce little or no amyloid-β (Roberds et al., 2001).

BACE is also responsible for cleavage of a Golgi-resident sialyltransferase (Kitazume et al., 2001), consistent with the localization of BACE primarily in the Golgi and endoplasmic reticulum (ER). Earlier studies suggest that amyloid-β can be generated in both the trans-Golgi network and endosomal pathways. It is not known if this reflects early BACE activity and trafficking of C99 or if BACE-APP interactions occur in multiple cell compartments. We tested the hypothesis that BACE can interact with APP at the cell surface and/or in early endosomes using a novel fluorescence energy transfer technique, co-immunostaining and pulse-chase experiments to examine the subcellular localization of APP-BACE interactions in living cells. Our results highlight a previously unemphasized APP-BACE interaction at the cell surface.

Materials and Methods

Generation of expression constructs and deletion mutants for human APP and BACE

Human APP770 cDNA lacking the termination codon was generated

by PCR and ligated in-frame to an expression vector pcDNA3.1B (Invitrogen, Carlsbad, CA) (APP770-myc). APP770-V5 construct was then made; ligated into the *Bam*HI and *Sac*II sites of pcDNA3.1/V5-His-TOPO vector (Invitrogen). Generation of APP770-GFP construct was described elsewhere (Kinoshita et al., 2001).

To make a Swedish mutant of APP, mutation of lysine residue at codon 670 and methionine residue at codon 671 to asparagine and leucine, respectively (of the 695 numbering), of the APP770-myc construct was accomplished using the QuickChange site-directed mutagenesis kit (Stratagene, La Jolla, CA). The presence of the Swedish mutation in APP770-myc (APPsw) was confirmed by DNA sequencing. An APP770myc construct that lacks the entire cytoplasmic region (APP770delta49) was made by PCR of the first 721 amino acids of APP770 with the primers 5′-ATAGCTAGCCAC-CATGCTGCCCGGTTTG-3′ and 5′-CGGAAGCTTCACCAAGGT-GATCACGAT-3′, and cloned into the *Nhe*I and *Hin*dIII sites of pcDNA3.1A myc/His (–) (Invitrogen).

BACE was cloned by PCR from the whole human brain cDNA library (Quick Clone cDNA; Clontech, Palo Alto, CA) using these primers: 5′-AGCCACCAGCACCACCAGACTTG-3′, 5′-ACTG-GTTGGTAACCTCACCCATTA-3′. The PCRed BACE clone was inserted into pcDNA3.1/V5/His-Topo vector (Invitrogen) (BACE-V5). To make the N-terminally myc-tagged BACE construct, the PCRed BACE fragment containing XhoI and XbaI sites at the ends was inserted into pSecTagN2myc plasmid (a gift from I. Mikhailenko, American Red Cross, Rockville, MD). Authenticity of the PCR-generated constructs has been confirmed by DNA sequencing. The constructs used in this study are summarized in Fig. 1.

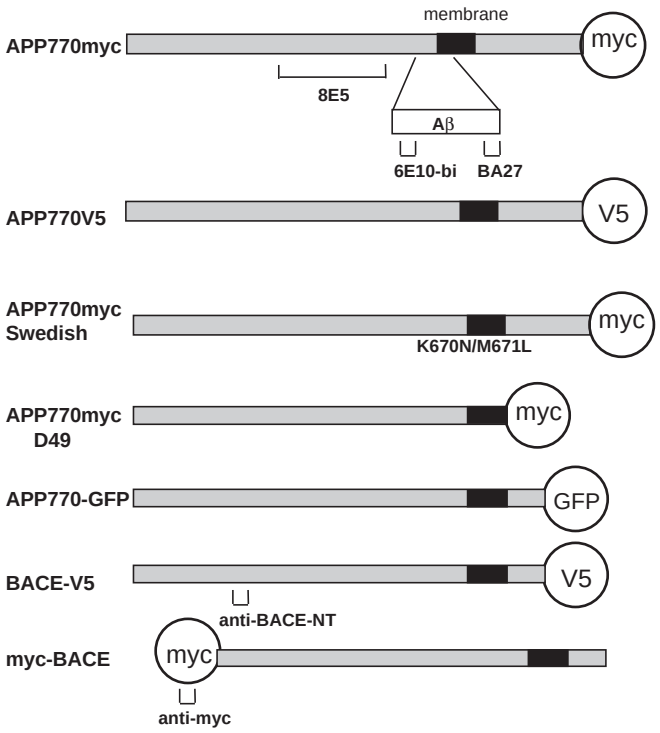

Fig. 1. Reagents used in this study. This scheme shows the constructs and antibodies used in this study. Membrane-spanning regions are shown in black. All APP constructs are tagged at the C-terminus with myc, V5 or EGFP; wild-type APP770, APP with Swedish mutant, APP delta49 which lacks the entire cytoplasmic domain. BACE constructs are either N-terminally tagged (with myc) or C-terminally tagged with V5. For labeling the ectodomain regions of APP and BACE, 8E5 and anti-myc antibody are used, respectively. For amyloid-β ELISA, biotinylated 6E10 and BA27 are used to capture amyloid-β.

Antibodies and reagents

Monoclonal antibody 8E5 was raised against the 520-668 amino acid residues of APP770 (a gift from P. Seubert, Elan Pharmaceuticals, South San Francisco, CA). Rabbit anti-BACE antibody raised against the N-terminus of BACE was obtained from Affinity Bioreagents (Golden, CO). Rabbit polyclonal anti-myc antibody and monoclonal anti-V5 antibody were purchased from Upstate Biotechnology (Lake Placid, NY) and Invitrogen, respectively. Antibodies against lysosomes (Lamp1 and biotinylated Lamp1), Golgi (GM130), and endosomes (EEA1 and FITC-conjugated EEA1) were obtained from BD Transduction Laboratories (San Diego, CA). For the amyloid-β ELISA study, biotinylated 6E10 (Signet Laboratories, Dedham, MA) raised against the N-terminus 17 amino acids of amyloid-β region was used for labeling and detection. An end-specific mouse monoclonal antibody BA27 (for Aβ40) or BNT77 raised against the 11-28 amino acid residues of amyloid-β was used for capturing (Takeda Chemical Industries, Tokyo, Japan). Secondary antibodies against mouse or rabbit IgG conjugated with Cy3 or FITC, respectively, were purchased from Jackson ImmunoResearch Laboratories (West Grove, PA). The gamma secretase inhibitor DAPT (Dovey et al., 2001) was a generous gift from M. Wolfe (Brigham and Women's Hospital, Boston, MA).

Cell culture conditions and transient transfection

H4 cells derived from human neuroglioma cells are used in this study (ATCC; Manassas, VA). H4 cells were cultured in OPTI-MEMI with 10% fetal bovine serum. Transient transfection of H4 cells was performed using a liposome-mediated method (FuGene 6; Roche Molecular Biochemicals, Indianapolis, IN). Cells were split into 4-chambered slides 1 day before the transfection. First, a mixture of 1 μg of plasmid DNA and 3 μl of FuGene6 was made in 100 μl of Dulbecco's modified Eagle's medium and left for 15-30 minutes at room temperature. Then 25 μl of this mixture was added to the medium in each well. The incubation time was from 24 hours to 48 hours. Double transfection of APP and BACE was performed in the same way.

Immunocytochemistry

Immunostaining was done on the cells 24-48 hours post-transfection. To detect the interactions in the secretory pathway, cells were fixed in 4% paraformaldehyde for 10 minutes, washed in Tris-buffered saline (TBS pH 7.3) and permeabilized by 0.5% Triton X-100 for 20 minutes, and blocked with 1.5% normal goat serum for 1 hour. To detect the interaction of APP and BACE on the cell membrane, a construct in which a myc epitope was present at the N-terminus of BACE was used. APP (wild-type or Swedish mutant) and BACE co-transfected cells were incubated with primary antibodies against the extracellular domain of APP (8E5) and rabbit anti-myc antibody in the culture media for 1 hour on ice, then washed with ice-cold PBS, and fixed in 2% PFA for 10 minutes. After washing in TBS 3 times, secondary antibodies conjugated with Cy3 or FITC were applied to visualize the primary antibodies without permeabilization.

Internalization assay

To investigate the interaction of APP and BACE in the endocytic pathway, we followed the method of APP internalization experiments developed by Yamazaki et al. (Yamazaki et al., 1996). To examine this interaction between APP and BACE, APP770-myc and BACE-V5-co-transfected H4 cells were surface-labeled with antibody against the ectodomain of APP (8E5, 1:1000) for 1 hour at 4°C in the culture media and washed with ice-cold PBS three times, then returned to 37°C for varying intervals; 0, 15, 30 and 60 minutes. Cells were then

fixed in 4% PFA for 10 minutes, permeabilized with 0.5% Triton X-100 for 5 minutes and applied with rabbit anti-BACE antibody against N-terminus portion of BACE. Then cells were incubated with appropriate secondary antibodies (Cy3 conjugated-anti-mouse and FITC conjugated-anti-rabbit antibodies, respectively; 10 μg/ml each) for 1 hour at room temperature. To confirm these results, co-transfected H4 cells were surface labeled by mouse monoclonal anti-APP 8E5 and rabbit anti-myc antibody (for N-terminally myc-tagged BACE construct) and both APP and BACE were internalized and examined in the same way as stated above.

For the triple labeling with the endosomal marker EEA1, cells were incubated in the primary antibodies against APP and BACE, followed by the secondary antibodies Cy5-conjugated anti-mouse IgG (to label APP) and Cy3-conjugated anti-rabbit IgG (to label BACE), and then FITC-conjugated EEA1 was added to label endosomes. For labeling with the lysosomal marker Lamp1, cells were first labeled with anti-APP (Cy5; 10 μg/ml) and anti-BACE (FITC), then incubated in biotinylated-Lamp1, followed by streptavidin-Cy3 (10 μg/ml; Jackson ImmunoResearch).

ELISA

To detect amyloid-β derived from cell surface APP, we labeled cells as above using biotinylated 6E10, an antibody directed against the amino terminal region of amyloid-β. The biotinylated-6E10-labeled-amyloid-β generated during the endocytosis experiment was assayed using a sandwich ELISA assay. The H4 cells were transfected with various constructs (APP770-myc, APP770-myc-Swedish, APP770delta49). DAPT (80 nM), the potent gamma secretase inhibitor was applied to some of the APP770(wild-type)-transfected H4 cells 3 hours after transient transfection. On the next day, the cells were labeled by incubating biotinylated-6E10 (1:100) in conditioned media at 4°C for 1 hour. The cells were then washed with ice-cold PBS 5 times, and replaced by fresh culture media containing 0.1% bovine serum albumin, then returned to 37°C for various intervals (0 minutes to 4 hours). The conditioned media was taken for ELISA every 30 minutes, then replaced by fresh media. The amount of amyloid-β from the conditioned media was measured in triplicate. Briefly, ELISA plates were coated with BA27 solution overnight. Then the conditioned media containing biotinylated-6E10-bound amyloid-β was added to the plate, washed with PBS and HRP-conjugated streptavidin was added. Fluorogenic substrate (QuantaBlu, PierceBiotechnology, Rockford, IL) was added and the fluorogenic product was read at excitation of 320 nm and at emission of 400 nm with a Wallac multiplate reader. The 6E10 cell-surface labeling was confirmed by immunostaining the cells at the noted timepoints. In a separate experiment, a β-galactosidase plasmid was co-transfected with these plasmids to normalize transfection efficiency.

FRET

Immunostaining was observed using a Bio-Rad 1024 confocal microscope mounted on a Nikon Eclipse TE300 inverted microscope; the krypton-argon laser (emission 488 nm and 568 nm lines) was used to excite the fluorescein or GFP and Cy3, respectively. FRET was measured using a method developed for laser scanning confocal microscopy (Knowles et al., 1999; McLean et al., 2000; Siegel et al., 2000; Kinoshita et al., 2001). The energy transfer was detected as an increase in donor fluorescence (FITC or GFP) after complete photobleaching of the acceptor molecules (Cy3). The amount of energy transfer was calculated as the percentage increase in donor fluorescence after acceptor photobleaching. An initial scan was obtained at low laser energy using the 488 line of the krypton-argon laser to record the fluorescein (or GFP) signal. A second scan was performed with the 568 line, and the area of co-localization was noted. A small part of the cell (approximately 5×5 μm) was then photobleached with brief exposure to intense 568-nm light (laser power 100%) to destroy the acceptor molecules. The cells were then re-scanned using 488-nm light. An increase of the fluorescein (or GFP) within the photobleached area was used as a measure of the amount of FRET present. The ratio Fl_{D2}/Fl_{D1} (in which Fl_{D2}/Fl_{D1} indicates the ratio of donor fluorescence after photobleaching to donor fluorescence before photobleaching, both corrected for background) was compared with the null hypothesis value of 1.0 by one group t tests. Comparison of multiple groups was by ANOVA, with Fisher's PLSD *post hoc* test for significance. FRET can be detected only if the two fluorophores are in close physical proximity: the distance between fluorophores must be less than ~10 nm. It should be noted that some groups normalize FRET measures to the final unquenched fluorescent intensity (e.g. Bastiaens et al., 1996); this would lead to a systematic change in the absolute values reported, but does not affect the rank order or relative difference of the FRET measures.

To detect APP-BACE interactions in the secretory pathway, FRET was examined in fixed H4 cells overexpressing APP770 (wild-type or Swedish mutant) and BACE using antibodies directed against their extracellular domains. For the cell surface and endocytosis studies, cells expressing BACE and APP were surface labeled as described above, then incubated at 37°C for various times, then labeled by FITC and Cy3, respectively. FRET between APP and BACE was examined at various times after returning the cells to 37°C (0, 15, 30 and 60 minutes) by fixing, then immunostaining and performing the co-localization and FRET proceedings as outlined above.

Positive and negative controls for FRET assays

A negative control for the FRET experiment is simply the absence of the acceptor (Cy3) fluorophore. Exposing singly labeled cells to 568 nm light for equivalent times did not alter the amount of fluorescein emission. In this case, Fl_{D2}/Fl_{D1} was 1.01±0.05 (mean±s.d.), indicating no FRET. Further negative controls for the FRET experiments include the following conditions: cells co-transfected with APP770-myc and APP770-V5 showed complete co-localization when immunostained with mouse anti-V5 (labeled by Cy3) and rabbit anti-myc (labeled by FITC) antibodies, but no FRET was observed (Fl_{D2}/Fl_{D1}=1.004±0.05, mean±s.d., n=12, not significant). APP770-GFP was co-transfected with APP770-myc and again there was complete overlap of the GFP and myc signals at the light level, but no FRET was observed (Fl_{D2}/Fl_{D1}=1.01±0.04, mean±s.d., n=12, not significant). APP770-GFP transfected cells were immunostained with anti-GM130 antibody (labeled by Cy3), which also showed strong co-localization in the secretory pathways. Again, FRET values were not different from 0, despite co-localization. The negative control in the endocytic pathway was done by using the cells transfected with APP770-myc, surface labeled using 8E5 (anti-N-terminal APP), followed by 37°C incubation for 15 minutes to allow endocytosis. Cells were then immunostained by anti-mouse IgG conjugated with Cy3, then anti-EEA-FITC antibody. APP signal showed striking co-localization with EEA in endosomes. Here a minimal degree of enhancements of signal, Fl_{D2}/Fl_{D1}=1.05±0.07 (mean±s.d., n=20, P=0.06) was observed.

The positive control for the FRET experiment was done in the following way: cells transfected with APP770-myc were fixed and incubated with mouse anti-myc antibody, then labeled with goat anti-mouse IgG conjugated with Cy3, followed by applying the donkey anti-goat IgG-conjugated with FITC. This positive control provides an 'upper limit' on the amount of FRET one might measure in these systems: this was shown to be Fl_{D2}/Fl_{D1}=1.57±0.11 (mean±s.d., n=12, P<0.0001).

Results

Interaction between APP and BACE on the cell surface and in the endocytic pathway

To identify the subcellular location of the interaction sites

between APP and BACE, we employed co-localization and FRET experiments. The approach, using antibodies directed against extracellular epitopes in live cell immunoassays, allowed examination of APP-BACE interactions on the cell surface and during endocytosis.

First, we examined the spatial relationship between APP and BACE on the cell surface and in the endocytic pathway. We found APP could be readily labeled on the cell surface of live cells with the ectodomain-specific antibody 8E5, but that the N-terminal BACE antibody did not label BACE well in unfixed, living cells, although cell-surface staining could be observed readily in fixed cells. We therefore used two approaches to examine APP-BACE interactions on the cell surface and in endocytic pathways. H4 cells co-transfected with APP770-myc and BACE-V5 were surface-labeled with mouse monoclonal 8E5 antibody against the ectodomain of APP by incubating for 1 hour at 4°C to allow binding of the antibody, returned to 37°C for varying intervals (0, 15, 30 and 60 minutes) to allow cellular-mediated internalization, and then fixed in 4% PFA and permeabilized. Rabbit polyclonal anti-BACE antibody against the extracellular region was then applied, followed by the secondary antibodies (Cy3-conjugated anti-mouse IgG and FITC-conjugated anti-rabbit antibody) to visualize the primary antibodies.

An alternative approach was also used. H4 cells were co-transfected with APP and N-terminally myc-tagged BACE construct, and then surface-labeled by mouse monoclonal anti-APP 8E5 and rabbit anti-myc antibody. APP and BACE were internalized and examined in the same way as stated above. Both approaches gave equivalent results. At time 0, APP showed a fine punctate staining pattern over the cell surface (Fig. 2). Cell surface APP was almost completely co-localized with BACE (Fig. 2). After 5-15 minutes incubation at 37°C, a fine granular staining appeared inside the cells together with weaker cell surface staining that remained completely co-localized for APP and BACE. These fine granules within the cytoplasm were EEA immunoreactive (Fig. 3), and are considered to be early endosomes (Yamazaki et al., 1996). APP and BACE showed complete co-localization in this compartment (Fig. 3). By 30-60 minutes, the vesicles appeared larger and coarser, and their distribution was distinctly perinuclear. At 60 minutes, cell surface staining was rarely observed, and most structures immunolabeled by anti-APP antibody are considered to be lysosomes, which was confirmed by anti-LAMP1 immunostaining (Fig. 3). APP and BACE co-localization was weaker at this timepoint (Fig. 3).

To test whether this co-localization suggested a close intermolecular proximity, we performed FRET assays. FRET, reflected by a ratio of Fl_{D2}/Fl_{D1} of greater than 1.0, can only be detected if the fluorophores are within 10 nm of each other. Positive and negative controls are described in the Materials and Methods section, and suggest that in this assay no interaction results in a ratio of 1.0, and a very strong interaction

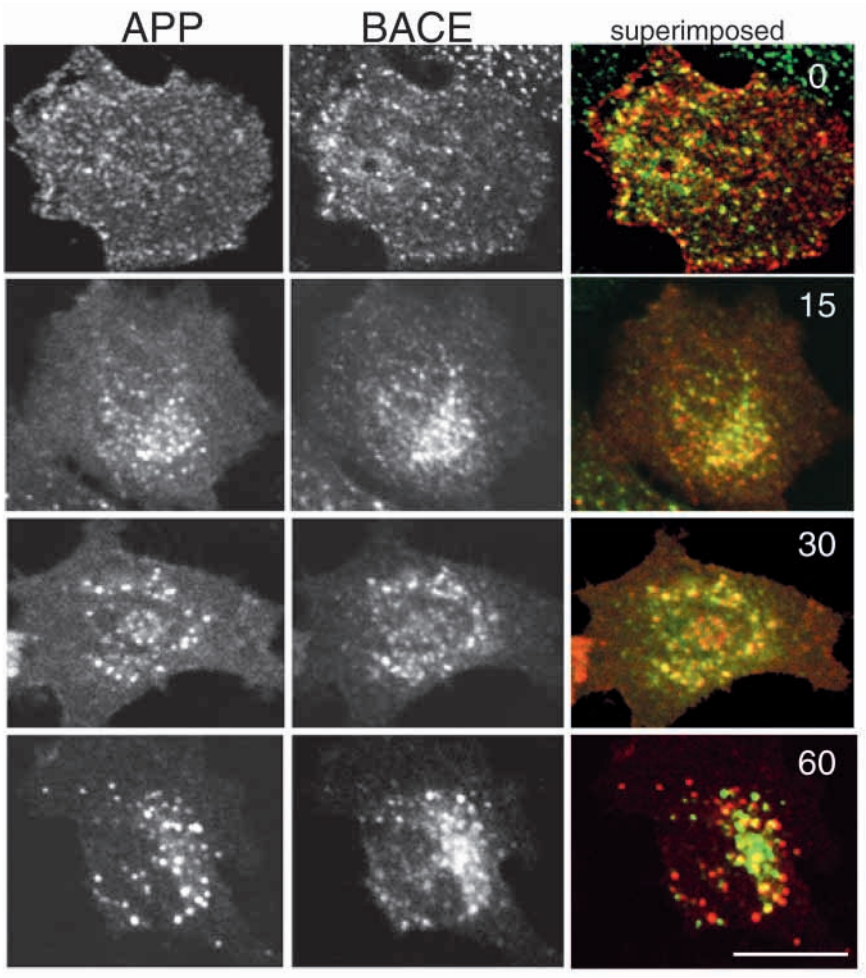

Fig. 2. Localization of APP and BACE on the cell surface and in the endocytic pathway. APP and BACE-co-transfected H4 cells were labeled by antibodies against extracellular regions (8E5 for APP, anti-myc for BACE) as described in the Materials and Methods section, and allowed to undergo endocytosis. They were fixed and permeabilized after 0, 15, 30 or 60 minutes, and the secondary antibodies were applied to detect the localization of the primary antibodies. At time 0 minutes, only the cell surface was labeled. Localization of APP and BACE are found in nearly identical clusters on the cell surface as shown in the bottom-right panel (APP in red, BACE in green). At 15-30 minutes, most signal was found in the endosomes, showing complete co-localization of APP and BACE signals. However, at 60 minutes, APP tended to localize in lysosomes, whereas BACE did not. Bar, 20 μm.

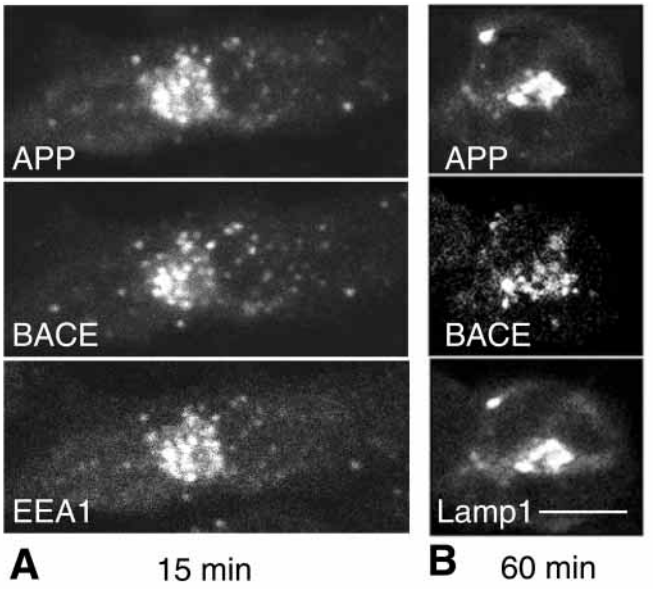

Fig. 3. Triple immunostaining of APP, BACE and endosomal (EEA1) (A)/lysosomal (Lamp-1) (B) markers. (A) Co-localization of APP and BACE in endosomes at 15 minutes. At 15 minutes, most signal was found in the endosomes (confirmed by EEA1 staining), showing complete co-localization of APP and BACE. (B) Distinct localization of APP and BACE at 60 minutes. APP signal was found mostly in lysosomes (confirmed by Lamp1), however BACE signal was not. Bar, 20 μm.

(antibody-antibody binding) gives a ratio of 1.57. Robust FRET was observed between APP and BACE on the cell surface (at time 0) (Fl_{D2}/Fl_{D1}=1.25±0.09, mean±s.d., n=15, P<0.0001) (Fig. 4), indicating that those two molecules directly interact with each other on the cell surface. Importantly, FRET was also detectable in the endosomes during endocytosis at 15-30 minutes (Fl_{D2}/Fl_{D1}=1.37±0.15, mean±s.d., n=45, P<0.0001, for 15 minutes, Fl_{D2}/Fl_{D1}=1.21±0.1, mean±s.d., n=51, P<0.0001, for 30 minutes) (Fig. 4A-E). At 60 minutes, APP signals that were localized mainly in the lysosomes were less co-localized with BACE signals, and there was no FRET between them in this compartment (Fl_{D2}/Fl_{D1}=1.02±0.03, n=10, not significant). FRET ratios were statistically significant between the cell surface and the endosomes (15 minutes) (P<0.05), and between early endosomes (15 minutes) and late endosomes (30 minutes) (P<0.001). Importantly, APPsw, known to be a better substrate for BACE, resulted in a substantially stronger amount of FRET with BACE on the cell surface (Fl_{D2}/Fl_{D1}=1.36±0.10, mean±s.d., n=10, P<0.0001). The difference between FRET ratio comparing APPwt and APPsw on the cell surface was also statistically significant (P<0.05).

Because the absolute value of FRET using the photobleach dequenching method is sensitive to fluorophore concentration, the results comparing cell surface to endosomal compartments do not clearly distinguish between a closer interaction or a larger number of molecules interacting. In either case, the data are clearly consistent with the hypothesis that APP encounters BACE on the cell surface and travels with it to the endosomes, but they do not interact in the lysosome.

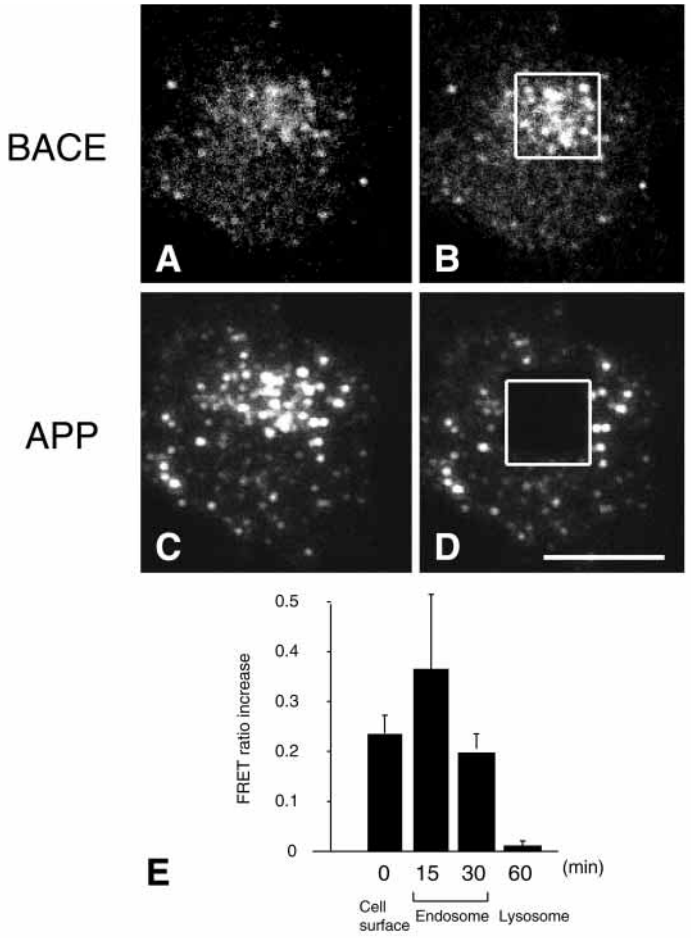

Fig. 4. Example of FRET reflecting the interaction between APP and BACE in the endosomes. (A-D) Example of FRET between APP-BACE in the endosomes. H4 cells were co-transfected with BACE-V5 (A,B) and APP-myc (C,D), immunostained with anti-APP antibody (labeled by Cy3) and anti-BACE antibody (labeled by FITC), both of which are directed against ectodomains. After labeling on ice, cells were incubated at 37°C for 15 minutes. Most of the APP signal was found in endosomes (confirmed by anti-EEA antibody), and co-localized with the BACE signal. Photobleaching of the Cy3 label of APP in the endosomes (D, boxed area) led to a marked increase in the BACE fluorescent signal within the photobleached area, demonstrating FRET (B, boxed area). Bar, 10 μm. (E) FRET ratio increases of Fl_{D2}/Fl_{D1} after photobleaching between APP and BACE in the secretory pathway, cell surface and endocytic pathway are shown. FRET measurements are shown for ectodomain interactions at 0 minutes after labeling (cell surface), 15-30 minutes after labeling (endosomes) and 60 minutes after labeling (lysosomes). FRET increases on the cell surface and in the endosomes were significantly above 1.0 (P<0.0001). FRET was not detected in the lysosomes.

APP-BACE interaction can also be detected in the secretory pathway

We also examined whether APP-BACE interactions could be detected in other cell compartments, using the fixed cells co-stained with 8E5 for APP and polyclonal anti-N-terminal antibody for BACE. Transfection with APPsw, known to be a better substrate for BACE, resulted in a substantially stronger

amount of FRET with BACE (1.19±0.03, mean±s.d., n=13, P<0.0001 for APPsw, 1.07±0.03, n=10, P<0.001 for wtAPP) in the secretory pathway including Golgi apparatus (confirmed by anti-GM130 antibody). APP-GM130 double staining showed co-localization at the light microscopic level, but no FRET (1.01±0.05, n=10, not significant).

Amyloid-β is generated in the endocytic pathway from cell surface APP

Cell surface labeling with APP and BACE N-terminal antibodies show that full-length APP associates with BACE at the cell surface. We next examined whether this cell surface APP was a substrate for BACE, and hence a source of amyloid-β generation, in our model system. To investigate how the interaction between APP and BACE impacts amyloid-β generation in the endocytic pathway, we pulse-labeled transfected H4 cells with biotinylated-6E10, then chased for up to 4 hours. The 6E10 labeling of the cell surface APP was confirmed by immunostaining. The conditioned media was collected and only the 6E10-labeled amyloid-β was measured by ELISA in order to identify the site of amyloid-β generation. As shown in Fig. 5A, the amyloid-β amount from the conditioned media was detected most during the first 30 minutes of chase. The amount of amyloid-β was measured for up to 4 hours, and gradually decreased over time. The same tendency was observed in APPsw-transfected H4 cells, although as expected, more amyloid-β was detected from the Swedish mutant. This result indicates that amyloid-β is rapidly generated on the cell surface or in the endosomes after pulse labeling of the cell surface. Next we compared the amyloid-β level from the various constructs in transfected H4 cells (Fig. 5B). Representative data of the relative ratio compared to the values of non-transfected H4 cells in one of the three experiments are shown. Swedish mutant APP showed increased generation of amyloid-β from 1.30±0.21 (wild-type APP, mean±s.d., n=3) to 1.85±0.2 (n=3) (Fig. 5A,B), whereas APP770 delta49, which lacks the entire cytoplasmic domain, showed decreased amyloid-β generation (from 1.30±0.21 to 1.09±0.02). Amyloid-β generation was inhibited to baseline by applying DAPT (1.06±0.1) (courtesy of M. Wolfe), a gamma secretase inhibitor. All the experiments were done three times each in triplicate and typical data are shown here.

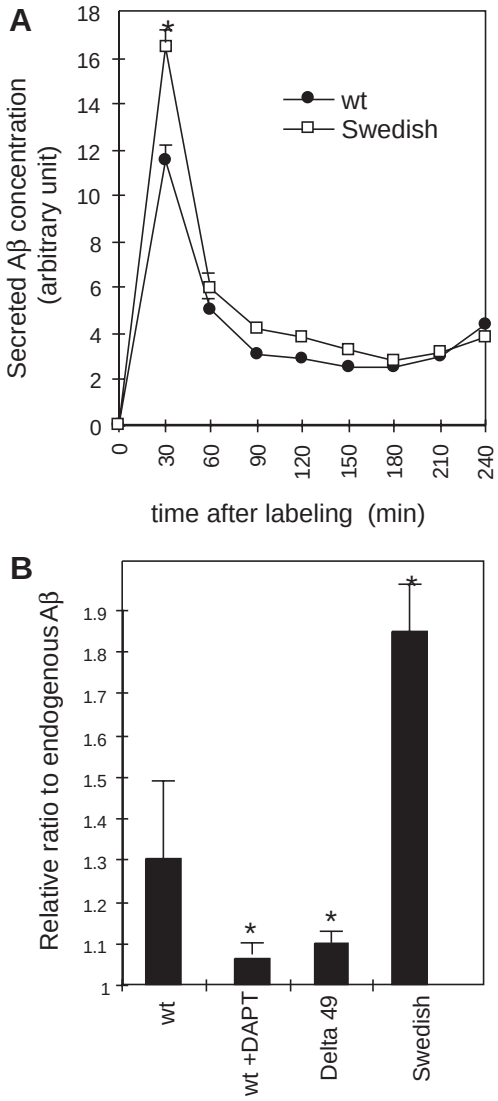

Fig. 5. Detection of amyloid-β peptide during endocytosis by ELISA. H4 cells transiently transfected with various APP constructs were pulse-labeled with biotinylated-6E10 and chased for the indicated time points in the absence or presence of DAPT for 4 hours. The conditioned media was collected and the biotinylated-6E10-labeled amyloid-β peptide was measured by ELISA using BA27 as the capture antibody and streptavidin-HRP for detecting labeled 6E10. (A) The time-course of amyloid-β detected from the conditioned media of wild-type APP770 and APP770sw-transfected H4 cells is illustrated. Data shown are typical of 3 separate experiments. (B) Comparison of the amyloid-β levels detected from various conditions (wt, Swedish, delta49, DAPT) for the first 30 minutes. A significant difference (P<0.001) in the amount of amyloid-β levels compared to that of the wild-type is shown by asterisk.

Discussion

Our current study provides morphological evidence from living cells testing the hypothesis that APP-BACE interactions occur at the cell surface and early endosomes. We found a surprisingly strong and previously unemphasized interaction at the cell surface, where APP and BACE dramatically co-localize and then appear to be internalized together into early endosomes.

It has previously been shown that amyloid-β can be generated from the Golgi/ER fractions (Kuentzel et al., 1993; Hartmann et al., 1997; Cook et al., 1997; Chyung et al., 1997) and so it has been assumed that BACE and APP interact there. Biochemical data also show that BACE interacts with Golgi-resident sialyltransferase (Kitazume et al., 2001) and with APP in a late Golgi compartment (Yan et al., 2001). Thus it is probable that APP and BACE interact at least in the Golgi, and our FRET analysis in fixed cells supports this conclusion. More surprisingly, our current experiments also demonstrate APP-BACE interactions at both the cell surface and in early endosomes. There is a dramatic co-localization of BACE and APP at the cell surface, as illustrated by cell surface labeling of live cells. This close interaction was confirmed by the demonstration of a strong FRET signal for APP-BACE

extracellular domains. The ELISA study detected measurable amounts of amyloid-β as early as 30 minutes after cell surface labeling, indicating that this interaction on the cell surface and early endosomes results in production of amyloid-β in our system. APP delta49, which is not internalized efficiently, generated less amyloid-β than wild-type APP. This result confirmed, in our system, that endocytosis may be an important step for amyloid-β production (Koo and Squazzo, 1994; Perez et al., 1999; Ulery et al., 2000).

A striking feature of our current studies is co-localization of APP and BACE at the cell surface in living cells (Fig. 2). Moreover, the presence of a detectable FRET signal, using the indirect immunofluorescent FRET technique that we have developed for in vitro studies (Kinoshita et al., 2001), suggests that the proteins are in close proximity. By contrast, co-localization by confocal microscopy suggests that proteins are (at best) within approximately 250 nm (half of the wavelength of light used for illumination). Thus, the FRET assay provides a finer resolution than simple co-localization, and strongly suggests a close intermolecular association at the cell surface.

We also studied BACE-APPsw interactions, because APPsw is believed to be a better substrate for BACE than wild-type APP. Enhanced FRET between APPsw and BACE confirmed the observation that APP and BACE interact in the Golgi apparatus and that APPsw interacts with BACE more strongly. Moreover, we demonstrated that APPsw demonstrated closer interaction with BACE on the cell surface by FRET measurement, and also gives rise to higher levels of amyloid-β from cell surface APP by ELISA, also implicating an effect of APPsw in the cell surface/endocytic pathway. These results are in excellent agreement with those from Perez et al. (Perez et al., 1996) and from Thinenkaran et al. (Thinenkaran et al., 1996), suggesting that APPsw leads to an increase in amyloid-β secretion from both the secretory and endocytic pathways. Other data suggest a predominance of APPsw amyloid-β generation in the secretory pathway (Haass et al., 1995; Citron et al., 1995; Steinhilb et al., 2002). Different techniques and cell preparations produced these results; our data suggest that in human H4 cells, APPsw and BACE interact in both secretory and cell surface/endocytic compartments.

Recent reports suggest that BACE protein level and activity are upregulated in Alzheimer disease brains (Fukumoto et al., 2002; Holsinger et al., 2002; Yang et al., 2003), supporting a role for BACE as an important therapeutic target. Identifying the cellular compartments in which BACE interacts with APP is of interest from the point of view of developing therapeutics. BACE is known to cleave APP in both position 1 of APP (the β site) and position 11 (the β′ site) of amyloid-β. One recent report suggests that, within the ER, β-site proteolysis predominates, whereas β′- is favored in the transGolgi network (Huse et al., 2002). Our data suggest that cell surface/early endosomal BACE activity leads to detectable levels of β-cleaved amyloid-β, because the assay depends on the presence of both the 6E10 site and the C-terminal BA27 site. The interaction of APP and BACE at the cell surface, prior to endocytosis, may thus impact amyloid-β production. The APP-BACE FRET assay may prove to be a useful tool for further analysis of these proteins' interactions and for screening molecules that potentially block their interactions at the cell surface in living cells.

We thank Hibiki Kawamata for assisting in the initial portion of this work. Michael Wolfe (Brigham and Women's Hospital, Boston, MA) generously provided DAPT, gamma secretase inhibitor. We thank M. Miyamoto (Takeda Chemical Industries, Tokyo, Japan) for ELISA reagents, I. Mikhailenko (American Red Cross, Rockville, MD) for pSecTagN2myc plasmid, and P. Seubert (Elan Pharmaceuticals, South San Francisco, CA) for antibody 8E5. Supported by NIH AG12406, AG15379, and P01AG05134.

References

Bastiaens, P. I. and Jovin, T. M. (1996). Microspectroscopic imaging tracks the intracellular processing of a signal transduction protein: fluorescent-labeled protein kinase C beta I. *Proc. Natl. Acad. Sci. USA* **93**, 8407-8412.

Bodendorf, U., Danner, S., Fischer, F., Stefani, M., Sturchler-Pierrat, C., Wiederhold, K.-H., Staufenbiel, M. and Paganetti, P. (2002). Expression of human beta-secretase in the mouse brain increases the steady-state level of beta-amyloid. *J. Neurochem.* **80**, 799-806.

Chyung, A. S., Greenberg, B. D., Cook, D. G., Doms, R. W. and Lee, V. M. (1997). Novel beta-secretase cleavage of beta-amyloid precursor protein in the endoplasmic reticulum/intermediate compartment of NT2N cells. *J. Cell Biol.* **138**, 671-680.

Citron, M., Teplow, D. B. and Selkoe, D. J. (1995). Generation of amyloid beta protein from its precursor is sequence specific. *Neuron* **14**, 661-670.

Cook, D. G., Forman, M. S., Sung, J. C., Leight, S., Kolson, D. L., Iwatsubo, T, Lee, V. M.-Y. and Doms, R. W. (1997). Alzheimer's Aβ(1-42) is generated in the endoplasmic reticulum/intermediate compartment of NT2N cells. *Nat. Med.* **3**, 1021-1023.

De Strooper, B. and Annaert, W. (2000). Proteolytic processing and cell biological functions of the amyloid precursor protein. *J. Cell Sci.* **113**, 1857-1870.

Dovey, H. F., John, V., Anderson, J. P., Chen, L. Z., de Saint Andrieu, P., Fang, L. Y., Freedman, S. B., Folmer, B., Goldbach, E., Holsztynska, E. J. et al. (2001). Functional gamma-secretase inhibitors reduce beta-amyloid peptide levels in brain. *J. Neurochem.* **76**, 173-181.

Fukumoto, H., Cheung, B. S., Hyman, B. T. and Irizarry, M. C. (2002). Beta-secretase protein and activity are increased in the neocortex in Alzheimer disease. *Arch. Neurol.* **59**, 1381-1389.

Haass, C., Lemere, C. A., Capell, A., Citron, M., Seubert, P., Schenk, D., Lannfelt, L. and Selkoe, D. J. (1995). The Swedish mutation causes early-onset Alzheimer's disease by beta-secretase cleavage within the secretory pathway. *Nat. Med.* **1**, 1291-1296.

Hartmann, T., Bieger, S. C., Bruhl, B., Tienari, P. J., Ida, N., Allsop, D., Roberts, G. W., Masters, C. L., Dotti, C. G., Unsicker, K. et al. (1997). Distinct sites of intracellular production for Alzheimer's disease A beta40/42 amyloid peptides. *Nat. Med.* 3, 1016-1020.

Holsinger, R. M., McLean, C. A., Beyreuther, K., Masters, C. L. and Evin, G. (2002). Increased expression of the amyloid precursor beta-secretase in Alzheimer's disease. *Ann. Neurol.* **51**, 783-786.

Huse, J. T., Liu, K., Pijak, D. S., Carlin, D., Lee, V. M.-Y. and Doms, R. W. (2002). β-secretase processing in the trans-Golgi network preferentially generates truncated amyloid species that accumulate in Alzheimer's disease brain. *J. Biol. Chem.* **277**, 16278-16284.

Kinoshita, A., Whelan, C. M., Smith, C. J., Mikhailenko, I., Rebeck, G. W., Strickland, D. K. and Hyman, B. T. (2001). Demonstration by fluorescence resonance energy transfer of two sites of interaction between the low-density lipoprotein receptor-related protein and the amyloid precursor protein: role of the intracellular adapter protein Fe65. *J. Neurosci.* **21**, 8354-8361.

Kitazume, S., Tachida, Y., Oka, R., Shirotani, K., Saido, T. C. and Hashimoto, Y. (2001). Alzheimer's beta-secretase, beta-site amyloid precursor protein-cleaving enzyme, is responsible for cleavage secretion of a Golgi-resident sialyltransferase. *Proc. Natl. Acad. Sci. USA* **98**, 13554-13559.

Knowles, R. B., Chin, J., Ruff, C. T. and Hyman, B. T. (1999). Demonstration by fluorescence resonance energy transfer of a close association between activated MAP kinase and neurofibrillary tangle: implications for MAP kinase activation in Alzheimer's disease. *J. Neuropathol. Exp. Neurol.* **58**, 1090-1098.

Koo, E. H. and Squazzo, S. L. (1994). Evidence that production and release of amyloid beta-protein involves the endocytic pathway. *J. Biol. Chem.* **269**, 21162-21166.

Kuentzel, S. L., Ali, S. M., Altman, R. A., Greenberg, B. D. and Raub, T. J. (1993). The Alzheimer beta-amyloid protein precursor/protease nexin-II

is cleaved by secretase in a trans-Golgi secretory compartment in human neuroglioma cells. *Biochem. J.* **295**, 367-378.

McLean, P. J., Kawamata, H., Ribich, S. and Hyman, B. T. (2000). Membrane association and protein conformation of a-Synuclein in intact neurons. *J. Biol. Chem.* **275**, 8812-8816.

Perez, R. G., Soriano, S., Hayes, J. D., Ostaszewski, B., Xia, W., Selkow, D. J., Chen, X., Stokin, G. B. and Koo, E. H. (1999). Mutagenesis identified new signals for b-amyloid precursor protein endocytosis, turnover, and the generation of secreted fragments, including Aβ42. *J. Biol. Chem*. **274**, 18851-18856.

Perez, R. G., Squazzo, S. L. and Koo, E. H. (1996). Enhanced release of amyloid beta-protein from codon 670/671 'Swedish' mutant beta-amyloid precursor protein occurs in both secretory and endocytic pathways. *J. Biol. Chem.* **271**, 9100-9107.

Roberds, S. L., Anderson, J., Basi, G., Bienkowski, M. J., Branstetter, D. G., Chen, K. S., Freedman, S. B., Frigon, N. L., Games, D., Hu, K. et al. (2001). BACE knockout mice are healthy despite lacking the primary beta-secretase activity in brain: implications for Alzheimer's disease therapeutics. *Hum. Mol. Genet.* **10**, 1317-1324.

Selkoe, D. J. (1998). The cell biology of the beta-amyloid precursor protein and presenilin in Alzheimer's disease. *Trends Cell Biol.* **8**, 447-453.

Siegel, R. M., Frederiksen, J. K., Zacharias, D. A., Chan, F. K., Johnson, M., Lynch, D., Tsien, R. Y. and Lenardo, M. J. (2000). Fas preassociation required for apoptosis signaling and dominant inhibition by pathogenic mutations. *Science* **288**, 2354-2357.

Sinha, S., Anderson, J. P., Barbour, R., Basi, G. S., Caccavello, R., Davis, D., Doan, M., Dovey, H. F., Frigon, N., Hong, J. et al. (1999). Protein purification and cloning of amyloid precursor protein beta-secretase from human brain. *Nature* **402**, 537-540.

Steinhilb, M. S., Turner, R. S. and Gaut, J. R. (2002). ELISA analysis of β-secretase cleavage of the Swedish amyloid precursor protein in the secretory and endocytic pathways. *J. Neurochem.* **80**, 1019-1028.

Thinenkaran, G., Teplow, D. B., Siman, R., Greenberg, B. and Sisodia, S. S. (1996). Metabolism of the 'Swedish' amyloid precursor protein variant in neuro2a (N2a) cells. Evidence that cleavage at the 'beta-secretase' site occurs in the Golgi apparatus. *J. Biol. Chem.* **271**, 9390-9397.

Ulery, P. G., Beers, J., Mikhailenko, I., Tanzi, R. E., Rebeck, G. W., Hyman, B. T. and Strickland, D. K. (2000). Modulation of beta-amyloid precursor protein processing by the low density lipoprotein receptor-related protein (LRP). Evidence that LRP contributes to the pathogenesis of Alzheimer's disease. *J. Biol. Chem.* **275**, 7410-7415.

Vassar, R., Bennett, B. D., Babu-Khan, S., Kahn, S., Mendiaz, E. A., Denis, P., Teplow, D. B., Ross, S., Amarante, P., Loeloff, R. et al. (1999). B-secretase cleavage of Alzheimer's amyloid precursor protein by the transmembrane aspartic protease BACE. *Science* **286**, 735-741.

Yamazaki, T., Koo, E. H. and Selkoe, D. J. (1996). Trafficking of cell-surface amyloid beta-protein precursor. II. Endocytosis, recycling and lysosomal targeting detected by immunolocalization. *J. Cell Sci.* **109**, 999-1008.

Yan, R., Bienkowski, M. J., Shuck, M. E., Miao, H., Tory, M. C., Pauley, A. M., Brashier, J. R., Stratman, N. C., Mathews, W. R., Buhl, A. E. et al. (1999). Membrane-anchored aspartyl protease with Alzheimer's disease beta-secretase activity. *Nature* **402**, 533-537.

Yan, R., Han, P., Miao, H., Greengard, P. and Xu, H. (2001). The transmembrane domain of the Alzheimer's beta-secretase (BACE1) determines its late Golgi localization and access to beta-amyloid precursor protein (APP) substrate. *J. Biol. Chem.* **276**, 36788-36796.

Yang, L.-B., Lindholm, K., Yan, R., Citron, M., Xia, W., Yang, X.-L., Beach, T., Sue, L., Wong, P., Price, D. et al. (2003). Elevated β-secretase expression and enzymatic activity detected in sporadic Alzheimer disease. *Nat. Med.* **9**, 3-4.